1032 *Chem. Mater.* **2010,** *22,* 1032–1037
DOI:10.1021/cm901910p

CHEMISTRY OF MATERIALS
Article

Sulfur-Tolerant Anode Catalyst for Solid Oxide Fuel Cells Operating on H_2S-Containing Syngas†

Cheng Peng,‡ Jingli Luo,* Alan R. Sanger, and Karl T. Chuang

Department of Chemical and Materials Engineering, University of Alberta, Edmonton, AB T6G 2G6, Canada. ‡ *Permanent address: School of Chemistry and Chemical Engineering, South China University of Technology, Guangzhou 510640, China*

Received July 2, 2009. Revised Manuscript Received October 10, 2009

Strontium-doped lanthanum vanadate, $La_{0.7}Sr_{0.3}VO_4$, LSV, was prepared via a nitrate-citrate combustion method. The phase formation process of LSV was studied using thermogravimetric analysis and X-ray diffraction (XRD). A pure phase of LSV was formed during baking at 900 °C for 7 h in 10% H_2−Ar. LSV is chemically and electrochemically stable in H_2S-containing syngas (40% H_2, 60% CO, and 5000 ppm H_2S). LSV is an active anode catalyst for use in solid oxide fuel cells (SOFCs), and a H_2-air fuel cell with configuration LSV/YSZ/Pt provided maximum power density of 210 mW cm^{-2} at 900 °C and a current density close to 400 mA cm^{-2}. Impedance measurements showed that the anodic polarization resistance depended on the fuel gas, and was highest for CO and lowest for H_2. The ohmic and polarization resistance of the cell decreased with increase in temperature.

1. Introduction

It is established that SOFCs are very promising energy conversion devices.[1] One of the most significant advantages of SOFCs is that alternative fuels other than pure hydrogen can be used because they are operated at a relatively high temperature.[2−4] However, one of the major challenges for extended fuel application in SOFC is anode poisoning caused by H_2S present in economically available hydrocarbon resource-derived fuels such as coal syngas, diesel, biogas, and sour gas.[5−8] At present, conventional Ni/YSZ composite cermet anodes for SOFCs have poor tolerance to even low amounts of H_2S in the fuel, and more than 100 ppm H_2S in the fuel can cause considerable loss in performance of Ni/YSZ anodes.[9,10] Therefore, H_2S-containing fuels used in SOFCs must be desulfurized, which increases both the complexity and cost of fuel systems and lower overall energy conversion efficiencies. Consequently, it is highly desirable to develop new anode materials with good sulfur tolerance as well as high catalytic activity. Several kinds of materials have been investigated as potential candidates for sulfur-tolerant anode in SOFCs and these materials can be classified mainly into three categories: (i) thiospinels and metal sulfides;[11,12] (ii) metal cermets; [13,14] and (iii) mixed ionic and electronic conductors (MIEC).[15,16]

To date, the search for sulfur-tolerant materials earlier investigation has focused on H_2S/air and molten carbonate fuel cells (MCFCs) system.[17−19] More recently, research interest included SOFC systems fed with H_2S-containing fuels.[20−23] However, there are few reports related to the application of H_2S−containing syngas as a feed gas in SOFCs.[24] Syngas is an important and

† Accepted as part of the 2010 "Materials Chemistry of Energy Conversion Special Issue".

*Corresponding author. Tel.: +001 780 492 2232. E-mail: jingli.luo@ualberta.ca.

(1) Minh, N. Q. *J. Am. Ceram. Soc.* **1993**, *76*(3), 563.
(2) Atkinson, A.; Barnett, S.; Gorte, R. J.; Irvine, J. T. S.; McEvoy, A. J.; Mogensen, M.; Singhal, S. C.; Vohs, J. *Nat. Mater.* **2004**, *3*(1), 17.
(3) Yates, C.; Winnick, J. *J. Electrochem. Soc.* **1999**, *146*(8), 2841.
(4) Sasaki, K.; Susuki, K.; Iyoshi, A.; Uchimura, M.; Imamura, N.; Kusaba, H.; Teraoka, Y.; Fuchino, H.; Tsujimoto, K.; Uchida, Y.; Jingo, N. *J. Electrochem. Soc.* **2006**, *153*(11), A2023.
(5) Moon, D. J.; Ryu, J. W. *Catal. Today* **2003**, *87*, 255.
(6) Sidwell, R. W.; Coors, W. G. *J. Power Sources* **2005**, *143*, 166.
(7) Herle, J. V.; Membrez, Y.; Bucheli, O. *J. Power Sources* **2004**, *127*, 300.
(8) Yaremchenko, A. A.; Valente, A. A.; Kharton, V. V.; Bashmakov, I. A.; Rocha, J.; Marques, F. M. B. *Catal. Commun.* **2003**, *4*, 447.
(9) Matsuzaki, Y.; Yasuda, I. *Solid State Ionics* **2000**, *132*, 261.
(10) Mukundan, R.; Brosha, E. L.; Garzon, F. H. *Electrochem. Solid-State Lett.* **2004**, *7*(1), A5.
(11) Vorontsov, V.; Luo, J. L.; Sanger, A. R.; Chuang, K. T. *J. Power Sources* **2008**, *183*(1), 76.
(12) Wang, S.; Liu, M.; Winnick, J. *J. Solid State Chem.* **2001**, *5*, 188.
(13) Tomita, A.; Tsunekawa, K.; Hibino, T.; Teranishi, S.; Tachi, Y.; Sano, M. *Solid State Ionics* **2006**, *177*, 2951.
(14) Ishihara, T.; Shibayama, T; Nishiguchi, H; Takita, Y. *Solid State Ionics* **2000**, *132*(3−4), 209.
(15) Cheng, Z.; Zha, S. W.; Aguilar, L.; Liu, M. L. *Solid State Ionics* **2005**, *176*, 1921.
(16) Huang, Y. H.; Dass, R. I.; Xing, Z. L.; Goodenough, J. B. *Science* **2006**, *312*, 254.
(17) Pujare, N. U.; Semkow, K. W.; Sammells, A. F. *J. Electrochem. Soc.* **1987**, *134*, 2639.
(18) Yentekakis, I. V.; Vayenas, C. G. *J. Electrochem. Soc.* **1989**, *136*(4), 996.
(19) Weaver, D.; Winnick, J. *J. Electrochem. Soc.* **1989**, *136*(6), 1679.
(20) Costa-Nunes, O.; Gorte, R. J.; Vohs, J. M. *J. Power Sources* **2005**, *141*, 241.
(21) Aguilar, L.; Zha, S.; Cheng, Z.; Winnick, J.; Liu, M. *J. Power Sources* **2004**, *135*, 17.
(22) Liu, M.; Wei, G. L.; Luo, J. L.; Sanger, A. R.; Chuang, K. T. *J. Electrochem. Soc.* **2003**, *150*(8), A1025.
(23) Lu, Y.; Schaefer, L. *J. Power Sources* **2004**, *135*, 184.
(24) Xu, Z. R.; Luo, J. L.; Chuang, K. T.; Sanger, A. R. *J. Phys. Chem. C* **2007**, *111*, 16678.

 Published on Web 10/29/2009

relatively inexpensive energy source. However, syngas normally manufactured by steam reforming of hydrocarbons may contain H_2S, derived from the sulfur content of the parent hydrocarbons. Thus development of anode materials which are both stable in H_2S-rich environments and catalytically active for conversion of syngas is indispensable for development of economically viable syngas SOFCs.

Lanthanum orthovanadates exhibit very interesting structural, electronic, magnetic, and electrical properties.[25,26] Recent efforts have focused on utilization of this material because of its catalytically active surface, for example, for vapor phase dehydrogenation of propane and selective oxidation of hydrogen sulfide.[27,28]

Herein we describe use of $La_{0.7}Sr_{0.3}VO_3$-based SOFC anode catalysts for oxidation of H_2S-containing syngas.

2. Experimental Section

$La_{0.7}Sr_{0.3}VO_3$ (LSV) powder was synthesized using a nitrate-citrate combustion method.[29] The starting materials were $Sr(NO_3)_2$ (Alfa Aesar, 99%), $La(NO_3)_3.6H_2O$ (Alfa Aesar, 99.9%), NH_4VO_3 (Alfa Aesar, 99%), and citric acid (Acros Organics, 99%). After combustion, the produced crude $La_{0.7}Sr_{0.3}VO_4$ powder was calcined at 700 °C for 1 h and subsequently reduced at 900 °C for 7 h in 10% H_2−Ar to form LSV.

The reaction of the $La_{0.7}Sr_{0.3}VO_4$ precursors and gel combustion to form a LSV powder product were investigated using thermogravimetric analysis (TGA) over the range 25−1400 °C with a TA SDT-Q600 instrument at a heating rate of 10 °C min^{-1} in air and 5% H_2/95% He mixture (flow rate: 100 mL min^{-1}).

Crystal phase identifications were performed using a Siemens D5000 X-ray diffractometer with Ni filtered Co K_α radiation. Morphology and microstructure of the samples as well as elemental analyses were determined using SEM/EDX techniques with a Hitachi S-2700 scanning electron microscope (SEM) and PGT Imix system with a PRISM IG.

Commercially available YSZ pellets (25 mm diameter and 0.3 mm thick; NexTech Materials. Ltd.) were used as the electrolyte. Porous platinum was used as cathode catalyst, prepared by screen printing platinum paste (Heraeus CL11−5100) to form a ca. 1 cm^2 circular electrode on one side of the YSZ pellet. After drying in air for 3 h, the pellet was then heated at 850 °C for 30 min to remove the organic medium and form the porous cathode. The LSV anode material was mixed with α-terpineol (Heraeus-372) to form a viscous paste that was screen printed on to the other side of the YSZ pellet and fired in situ at 900 °C in hydrogen atmosphere to form approximately 0.1 mm thick circular 1 cm^2 anodes. There was no electrode covering the areas adjacent the perimeters of each side of the electrolyte disks.

Current collectors comprising gold mesh welded to Au lead wires were placed in intimate contact with the surface of each electrode. The membrane electrode assemblies (MEA) so formed were secured between the outer of two coaxial alumina tubes on each side of the MEA to form the anode and cathode compartments. Ceramic sealant (Ceramabond 503, Aremco) was applied adjacent the perimeters of both sides of the electrolyte to seal the gas compartments. The cell was heated to selected temperatures in a tubular furnace (Thermolyne F79300). Air and N_2 initially flowed through the cathode and anode chambers, respectively. After the operating temperature had been reached, the N_2 stream was switched to H_2S-containing syngas.

A Solartron electrochemical interface (S1 1287) was used in all of the tests to monitor the open circuit voltage (OCV) between anode and cathode, and to measure current−potential performance and electrochemical impedance. Potentiodynamic mode was used when performing current−potential measurements. The scanning rate was kept at 5 mV/s. Impedance data were obtained over the frequency range 1 MHz to 0.1 Hz. The cell was allowed to equilibrate and stabilize until OCV had achieved a stable value after each change in operating conditions before conducting further measurements.

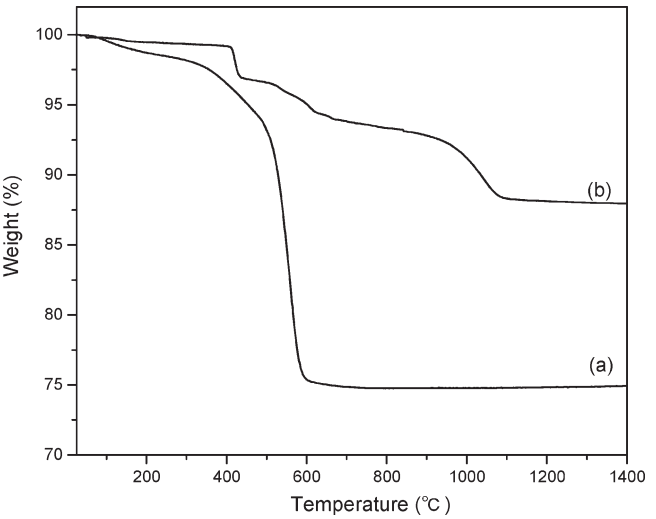

Figure 1. TGA curves for the $La_{0.7}Sr_{0.3}VO_4$ precursors of products from (a) gel combustion, and (b) conventional solid-state reaction.

3. Results and Discussion

3.1. Thermogravimetric Analysis and Phase Structure. TGA was used to examine the thermal changes during synthesis of the $La_{0.7}Sr_{0.3}VO_4$ samples prepared by gel combustion, and compare these properties with samples of mixtures of precursors for preparation of LSV by solid-state reaction (Figure 1). The overall weight loss during the conventional solid-state reaction was less than 15% and was complete around 1200 °C. In contrast, the overall weight loss was more than 30% for combustion of the gel, and the weight loss was completed by 728 °C. Thus the temperature for completion of weight loss was considerably lower for gel combustion than for the solid-state reaction, indicating that preparation of crude $La_{0.7}Sr_{0.3}VO_4$ using the nitrate−citrate combustion method requires lower temperatures than the solid-state reaction.

The $La_{0.7}Sr_{0.3}VO_4$ crystalline phase developed as the gel combustion product was baked in air for 1 h at 700 °C (X-ray crystallography; Figure 2). The gel combustion product had only weak crystallinity of the $La_{0.7}Sr_{0.3}VO_4$ perovskite phase, whereas the material was strongly

(25) Yan, J. Q.; Zhou, J. S.; Goodenough, J. B. *Phys. Rev. Lett.* **2004**, *93*, 235901.
(26) De Raychaudhury, M.; Pavarini, E.; Andersen, O. K. *Phys. Rev. Lett.* **2007**, *99*, 126402.
(27) Fang, Z. M.; Hong, Q.; Zhou, Z. H.; Dai, S. J.; Weng, W. Z.; Wan, H. L. *Catal. Lett.* **1999**, *61*, 39.
(28) Li, K. T.; Chi, Z. H. *Appl. Catal., A* **2001**, *206*, 197.
(29) Peng, C.; Zhang, Z. *Ceram. Int.* **2007**, *33*(6), 1133.

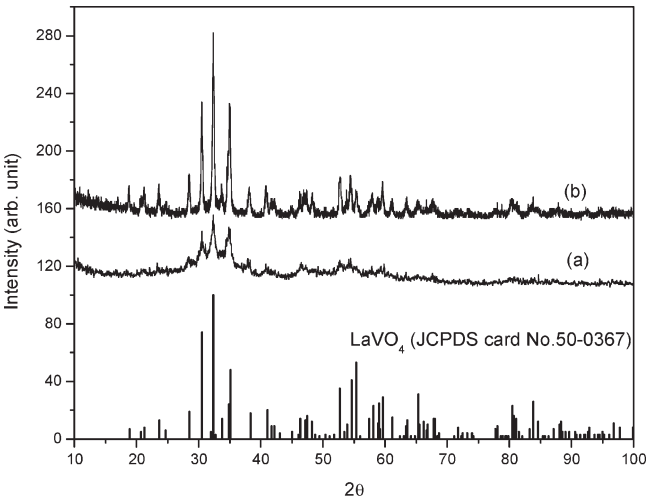

Figure 2. Thermal evolution of the powder X-ray diffraction spectrum of the $La_{0.7}Sr_{0.3}VO_4$: (a) combustion powder; (b) combustion powder after being heated at 700 °C for 1 h in air.

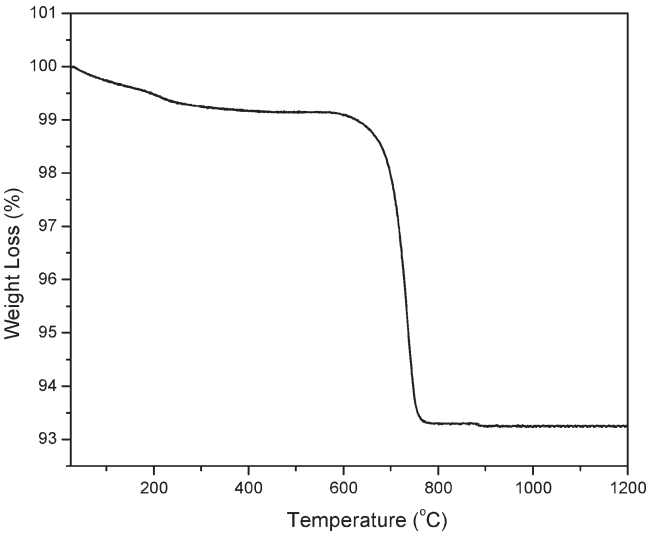

Figure 3. TGA of the gel combustion powder after being heated at 700 °C for 1 h.

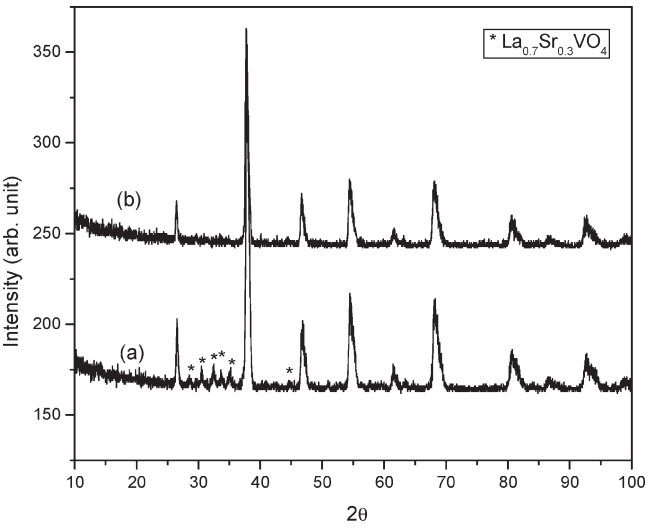

Figure 4. Thermal evolution of the powder X-ray diffraction spectrum of the LSV after being reduced in 10% H_2−Ar atmosphere: (a) 900 °C for 4 h; (b) 900 °C for 7 h.

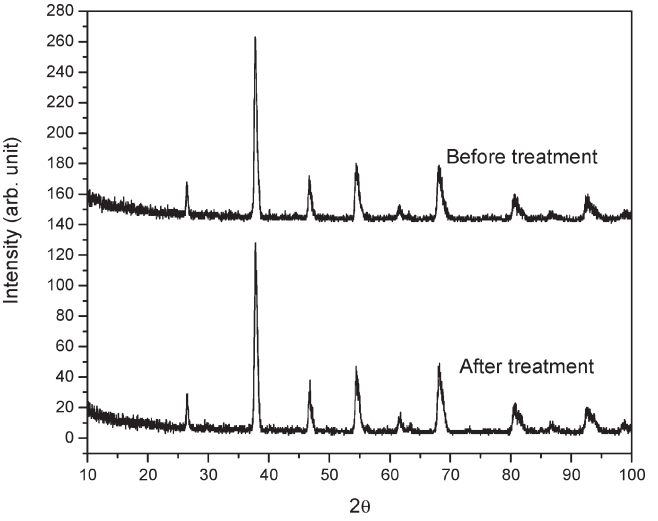

Figure 5. XRD patterns of LSV catalyst before and after exposure to H_2S-containing syngas at 900 °C for 72 h.

crystalline after calcining at 700 °C for 1 h. All the peaks were indexed by comparison with the monoclinic perovskite-type structure of lanthanum vanadate, $LaVO_4$, (JCPDS card no. 50−0367), which is a thermodynamically more stable state than the tetragonal perovskite-type structure [30]. Thus a pure perovskite phase was formed completely within 1 h at 700 °C, which is a much lower temperature than that required for synthesis of highly crystalline $La_{0.7}Sr_{0.3}VO_4$ by conventional solid-state reaction (greater than 1000 °C).[31]

The transformation of $La_{0.7}Sr_{0.3}VO_4$ into $La_{0.7}Sr_{0.3}VO_3$ during heating of the gel combustion powder at 700 °C for 1 h in H_2 atmosphere was monitored using TGA (Figure 3). Total transformation of $La_{0.7}Sr_{0.3}VO_4$ into $La_{0.7}Sr_{0.3}VO_3$ was complete around 900 °C, which indicated that 900 °C was an appropriate heat-treatment temperature for reduction in H_2. Interestingly, TGA showed a multiple-step process. The first step of weight loss below 200 °C was ascribable to the vaporization of physically absorbed and structural water. The other two weight losses (around 600 and 880 °C) were ascribed tentatively to successive reduction of V^{5+} to V^{4+} and V^{4+} to V^{3+} by loss of oxygen ions through reduction with H_2. To achieve charge balance, vanadium ions in $La_{1-x}Sr_xVO_3$ were reduced to either a mixture of V^{5+} and V^{3+}, or V^{4+}, or a mixture of all these valence states. In each case, there was a significant concentration of reduced vanadium ions in LSV.[32,33]

The as-synthesized $La_{0.7}Sr_{0.3}VO_4$ powder was baked in 10% H_2−Ar atmosphere at 900 °C for different times to investigate the evolution of the crystalline phase of $La_{0.7}Sr_{0.3}VO_3$ (X-ray diffraction; Figure 4). After baking at 900 °C for 4 h, the main diffraction peaks corresponded

(30) Fan, W.; Song, X.; Sun, S.; Zhao, X. *J. Solid State Chem.* **2007**, *180*, 284.
(31) Bashir, J.; Nasir Khan, M. *Mater. Lett.* **2006**, *60*, 470.
(32) Dougier, P.; Casalot, A. *J. Solid State Chem.* **1970**, *2*, 396.
(33) Hui, S.; Petric, A. *Solid State Ionics* **2001**, *143*, 275.

to indexed diffraction peaks for $LaVO_3$ (JCPDS card no. 33−0728), with residual peaks for the $La_{0.7}Sr_{0.3}VO_4$ phase (marked by asterisks in Figure 4), so the transformation of $La_{0.7}Sr_{0.3}VO_4$ into $La_{0.7}Sr_{0.3}VO_3$ was incomplete. After 7 h, only the peaks for a single LSV phase were found, and so the reaction was complete.

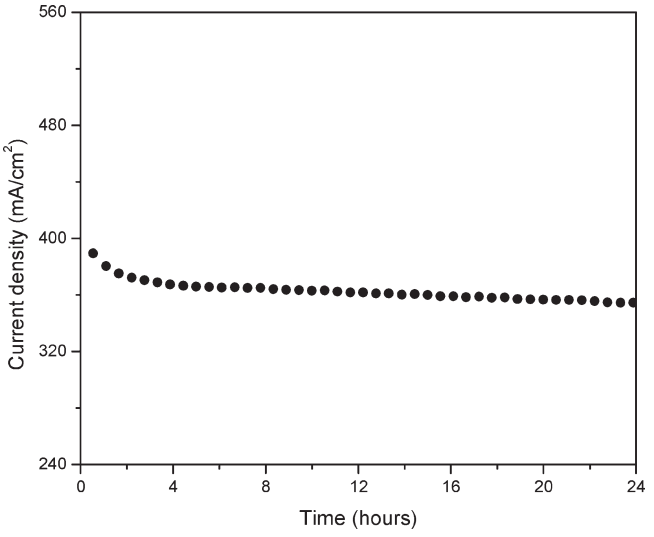

Figure 6. Electrochemical stability test curve for LSV/YSZ/Pt single cell. Cell was operated at V_{cell}, 0.5 V; T, 900 °C; P, 1 atm.

3.2. Stability of $La_{0.7}Sr_{0.3}VO_3$ in H_2S-Containing Syngas. The desired sulfur tolerant anode catalyst for syngas SOFCs must be both chemically and electrochemically stable in H_2S-containing atmospheres. To determine the chemical stability of LSV, a sample was baked in syngas (40% H_2, 60% CO, and 5000 ppm H_2S) at 900 °C for 72 h. After heating LSV in H_2S-containing syngas for up to 72 h there were no new phases detected in the XRD (Figure 5), showing that the material was chemically stable in the H_2S-containing syngas.

A potentiostatic study showed steady state performance of the catalyst in syngas (40% H_2, 60% CO, and 5000 ppm H_2S) at 900 °C over 24 h (Figure 6), showing that LSV was electrochemically stable under these conditions. The initial high currents corresponded largely to double-layer charging. The current density then decayed hyperbolically over 3 h, after which there was only a minor decline over the subsequent 21 h. The degradation rate of the cell performance was ca. 1.3% h^{-1}, which appeared to be due to the coarsening of the electrode and not to poisoning by H_2S. Figure 7 shows the cross-section SEM micrograph and EDX analyses for the LSV anode catalyst before and after 24 h tests in H_2S-containing syngas at 900 °C. Before each stability test the grain size of the anode catalyst was in the range 100−300 nm, with good porous structure. After each 24 h stability test, the

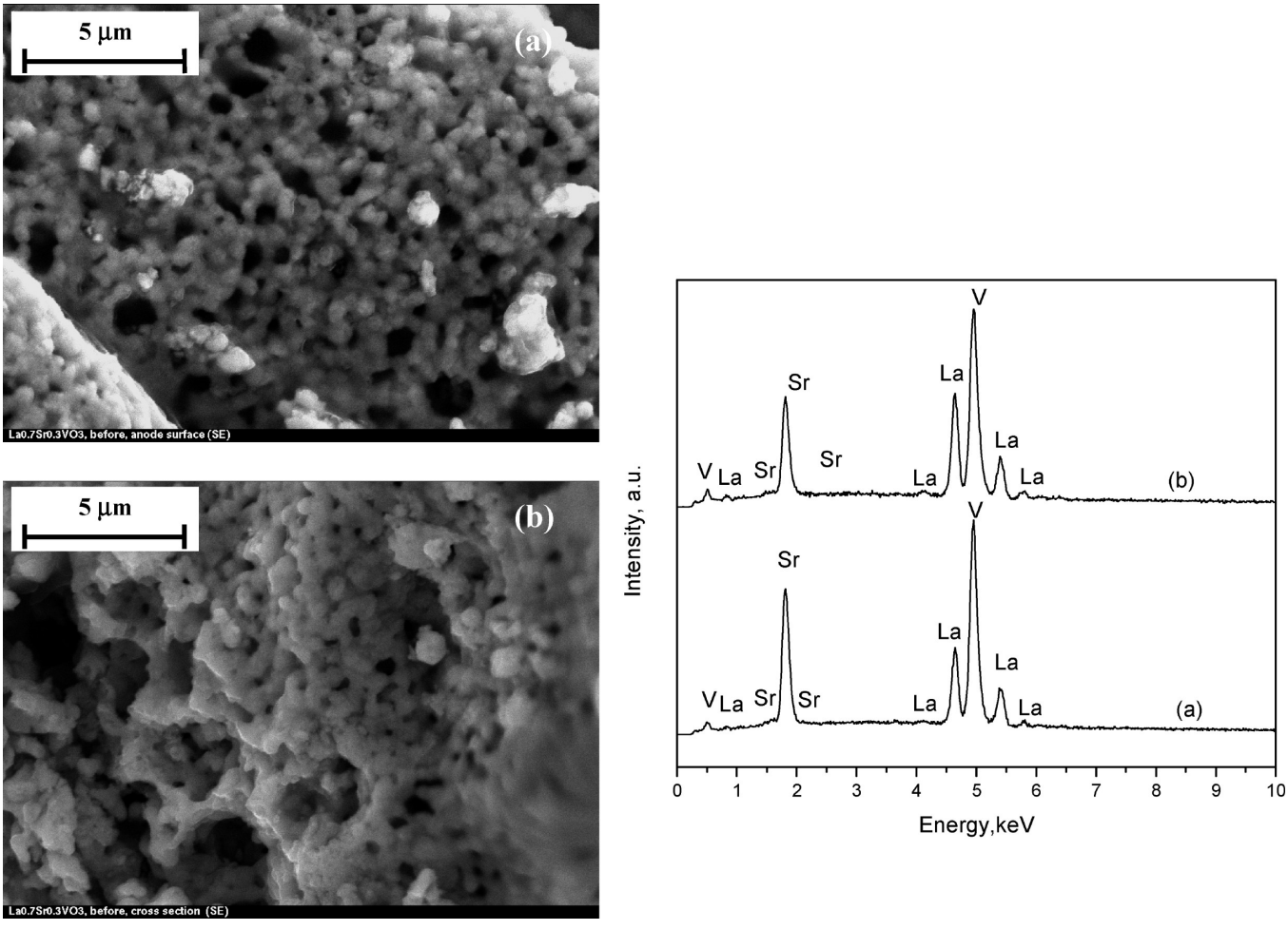

Figure 7. Cross-sectional SEM images and EDX analyses of the LSV anode catalyst (a) before and (b) after stability test.

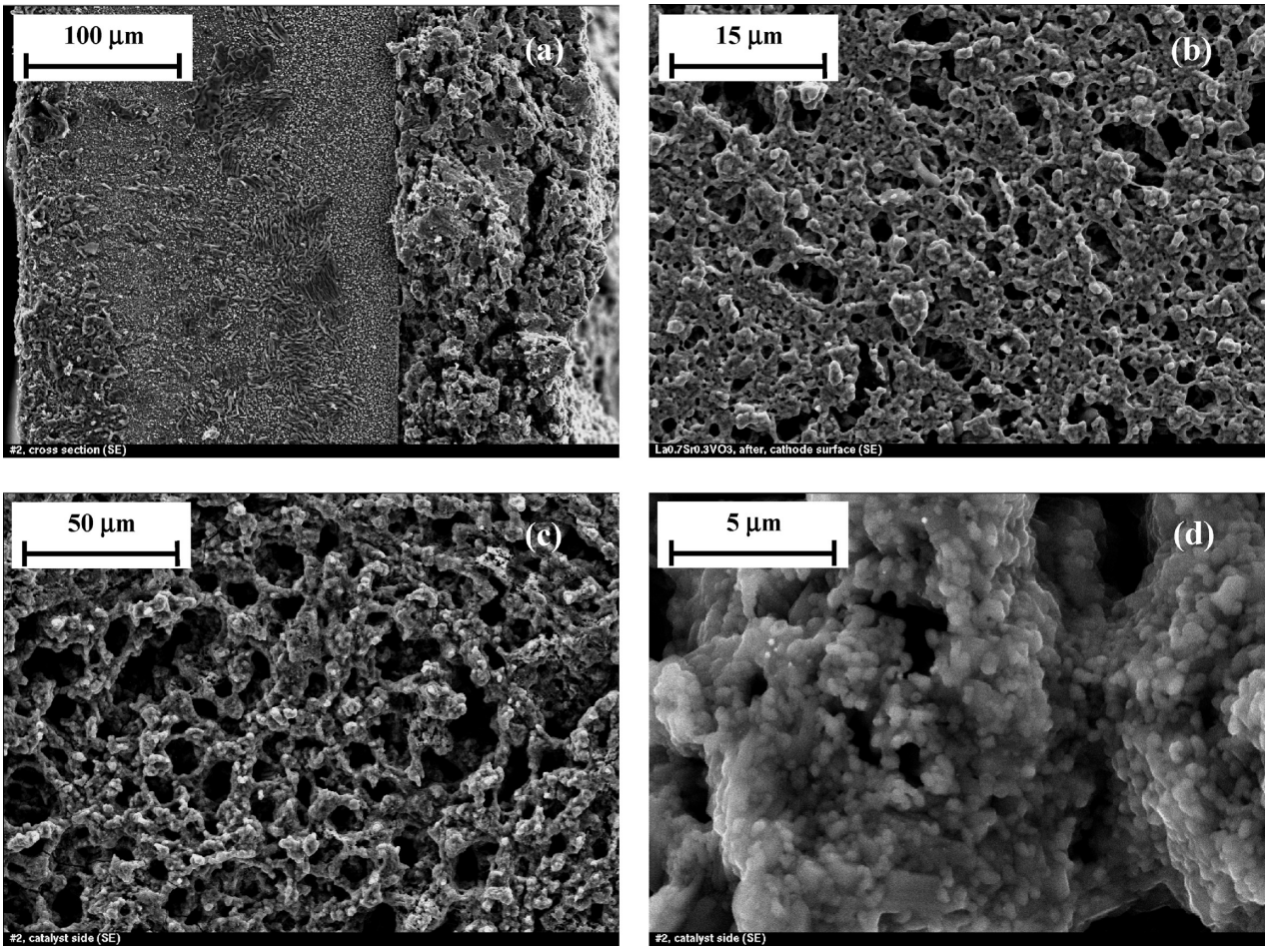

Figure 8. SEM images of (a) the assembly cross-sectional view, (b) top view of the cathode catalyst, and (c, d) the anode catalyst.

grains were larger and had poorer porous structure. EDX spectra showed that no carbon or sulfur was deposited on the surface of anode catalyst during stability tests, which showed that the LSV anode catalyst was not prone to the problems associated with use of Ni cermets in H_2S-containing syngas, and that the LSV anodes exhibited good sulfur tolerance in SOFC operated using H_2S-containing syngas as fuel.

3.3. Microstructure and Performance of the Single Cell Assembly. Figure 8 gives the overall cross-sectional view of a fractured cell. The thickness of the anode catalyst layer was approximately 100 μm. The cathode catalyst layer was very thin compared to the thickness of the anode layer. The cathode and anode catalysts each had uniform porous microstructure (images b and c in Figure 8), which provided better access to the full surface area and facile mass transfer within the catalyst layers. The particle size distribution for the anode catalyst was very narrow and the average particle size was around 200 nm.

The impedance spectra of single cells using LSV anodes operated using different fuels at 800 °C each consisted of two semicircles (Figure 9). Similar results were obtained at 850 and 900 °C. The high-frequency intercept of the semicircle near the origin of the plot corresponded to the ohmic resistance. The first semicircle at the high frequency was substantially similar for each of the fuel gases.

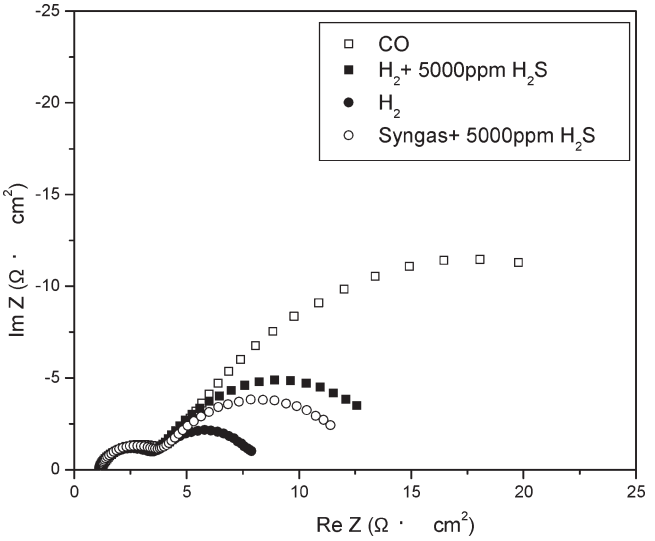

Figure 9. Impedance spectra for a fuel cell operated with different fuels at 800 °C.

However, the second, low-frequency semicircle varied considerably with change in fuel. Thus the two semicircles were ascribed to the cathodic polarization process and the anodic polarization process, respectively. The polarization radius for the cathode process was smaller than that for anodic polarization for each fuel. There was a significant effect of fuel gas on the anodic polarization

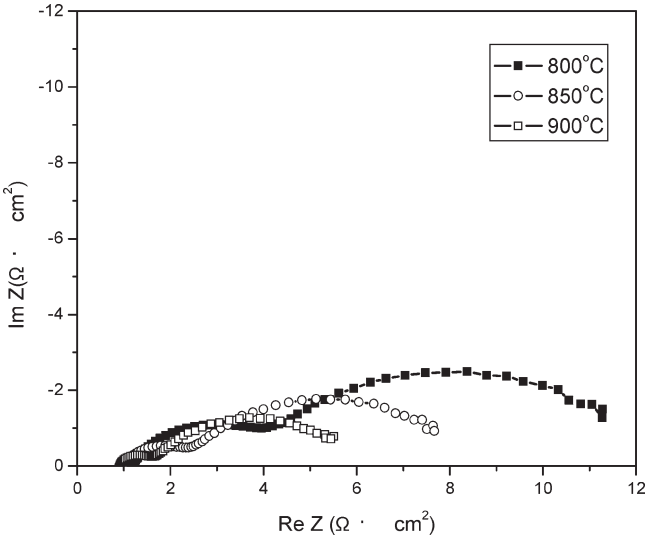

Figure 10. Impedance spectra of a fuel cell using H_2S-containing syngas as fuel operated at different temperatures.

process, and the largest anodic polarization resistance was for CO and the lowest anodic polarization resistance was for H_2 .

The impedance spectra of a single cell using H_2S-containing syngas as fuel varied with temperature (Figure 10). The ohmic resistance decreased with increase in temperature, for two reasons. The conductivity of the YSZ membrane increased with temperature. The contribution from the conductivity of LSV also increased, as it was a semiconductor at high temperatures in a reducing atmosphere.[20] Consequently, the radius for both semicircles decreased when temperature was increased, as polarization resistance for cathode and anode both decreased with increasing temperature and so, for both anode and cathode, the smallest polarization radii were obtained at 900 °C.

Fuel-cell performance using H_2S-containing syngas as fuel improved with temperature in the range 800−900 °C (Figure 11), consistent with the impedance measurements (Figure 10) which showed that ohmic and polarization resistance both decreased with increasing temperature. The maximum power density, 210 mW cm^{-2}, was obtained at 900 °C at a current density ca. 400 mA cm^{-2} and potential ca. 0.55 V. Activation polarization had a relatively lower impact on performance of the cell than ohmic and concentration polarizations under our operating conditions. The maximum power densities for each temperature were obtained in the potential range 0.5−0.55 V, in the ohmic polarization zone.

The OCV values were 1.161 at 800 °C, 1.149 at 850 °C, and 1.137 V at 900 °C, each of which was intermediate between the theoretical OCV values for H_2 and CO oxidation, which was consistent with our previous proposed reaction scheme for the same fuel gas under same operating condition using a different anode.[33] Therefore, the oxidation reactions for H_2 and CO in the cell had a predominant contribution to the overall OCV, not H_2S oxidation, and so the anode was effective for conversion of syngas as fuel even in the presence of H_2S.

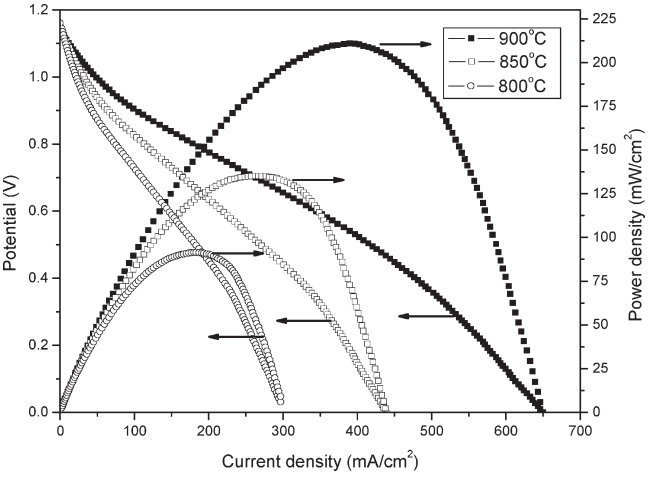

Figure 11. IV-IP performance of a fuel cell using H_2S-containing syngas as a fuel gas operated at different temperatures. Flow rate for fuel gas and air each 50 sccm.

4. Conclusions

The perovskite oxide $La_{0.7}Sr_{0.3}VO_3$ (LSV) was synthesized using a nitrate-citrate combustion method followed by reduction in H_2−Ar. The phase formation process of the monoclinic perovskite-type structure of $La_{0.7}Sr_{0.3}VO_4$ was complete by 700 °C, a much lower temperature than that required for conventional solid state synthesis (greater than 1000 °C).

$La_{0.7}Sr_{0.3}VO_4$ was fully reduced to LSV during reduction at 900 °C for 7 h in 10% H_2−Ar.

The XRD pattern of the catalyst before and after heating in H_2S-containing syngas for up to 72 h showed no new phases.

The potentiostatic study showed only a slight decline in output over a 24 h test period. The degradation rate 1.3% h^{-1} was attributable to coarsening of the electrode and not to poisoning of the catalyst; no sulfur or carbon was deposited on the anode.

LSV was active as an anode material for SOFCs operating in H_2S-containing syngas. The maximum power density, 210 mW cm^{-2}, was obtained at 900 °C at a current density close to 400 mA cm^{-2} and a potential of 0.55 V. Therefore, LSV is a promising candidate for anode material in SOFCs operating with H_2S-containing syngas as fuel.

The anodic polarization resistance of LSV varied with the fuel, and was largest for CO and lowest for H_2.

Acknowledgment. This work was supported by Natural Sciences and Engineering Research Council of Canada (NSERC) Strategic Project Grant.

Note Added after ASAP Publication. There were minor text errors in the version published ASAP October 29, 2009; the corrected version was published ASAP November 4, 2009.